

Impurity immersed in a two-component few-fermion mixture in a one-dimensional harmonic trap

Marek Teske¹ and Tomasz Sowiński¹

¹*Institute of Physics, Polish Academy of Sciences,
Aleja Lotników 32/46, PL-02668 Warsaw, Poland*

We investigate a one-dimensional three-component few-fermion mixture confined in a parabolic external trap, where one component contains a single particle acting as an impurity. Focusing on the many-body ground state, we analyze how the interactions between the impurity and the other components influence the system's structure. For fixed interaction strengths within the mixture, we identify a critical interaction strength with the impurity for which the system undergoes a structural transition characterized by substantial change in its spatial features. We explore this transition from the point of view of correlations and ground-state susceptibility. We remarkably find that this transition exhibits unique universality features not previously observed in other systems, highlighting novel many-body properties existing in multi-component fermionic mixtures.

I. INTRODUCTION

One of the most amazing puzzles of nature is the collective manifestation of quantum phenomena in the macroworld. Spectacular examples of such behaviour include the superfluidity [1, 2], the superconductivity [3, 4], the fractional quantum Hall effect [5], or the existence of giant magnetoresistance [6, 7]. On the phenomenological level, collectivity relies on the amplification of quantum effects caused by quantum statistics and mutual interactions of individual particles when their number becomes macroscopic. In this case, the complex microscopic description can be effectively replaced by a mesoscopic one that, on the one hand, ignores the exact knowledge of the individual particles while still partially accounting for their properties and interactions. This approach stands behind all approximate methods based on the mean-field theory [8–10], the density functional approach [11], or the renormalization group schemes [12].

The precise study of mesoscopic quantum systems can be very fruitful in itself [13]. This has become particularly appealing in the last two decades due to the development of extremely precise experimental possibilities for preparing and controlling systems containing a small number of strongly interacting ultracold atoms [14–16]. Thanks to a very high tunability, in such systems it is possible not only to control the number of particles precisely but also the strength of the interactions between them, the geometry of the external potential, and the effective dimensionality. As a result, a remarkable avenue to explore non-classical correlations in mesoscopic-sized systems has been opened [17–19]. As examples among others, let us mention here such phenomena as the spontaneous emerging of pairing in mesoscopic systems [20, 21], or the emergence of Pauli crystals [22, 23].

The experimental study of ultracold gases has opened up many new possibilities for discovering previously not well-known quantum phenomena. This is due to the possibilities offered by the rich internal structure of the

atoms. In particular, the existence of metastable atomic states with high total spin allows one to study exotic mixtures of quantum particles obeying various quantum statistics and experiencing highly non-trivial couplings between spin and spatial degrees of freedom [24–26]. Their properties in reduced dimensionality have become the subject of intensive research at many levels [27–36] but their collective behavior induced by interactions in the few-body regime still require systematic investigation.

In this work, we analyze a mesoscopic fermionic mixture consisting of three distinguishable components. Our aim is to test whether any collective effects may appear in the case of a larger number of components, which are not present in binary mixtures. In order to make these studies well-defined, reasonably comprehensive, and also going beyond extensively studied balanced mixtures, we consider the smallest possible extension of two-component fermionic mixture by introducing additional interaction with a single third-component particle. We aim to investigate if and how interactions with this impurity change the internal properties of the mixture. Moreover, we inspect non-classical correlations this may induce. In this way we also link our work to the well-studied problem of a single impurity interacting with several spin-polarized fermions [16, 37].

Our work is organized as follows. In Sec. II we introduce the theoretical model of the system studied and we describe its Hamiltonian in the convenient formalism. Then in Sec. III we briefly explain the exact diagonalization method in the energy cut-off framework. In Sec. IV we analyze single- and two-particle density distributions and we identify a specific transition in the many-body ground state of the system induced by interactions with impurity. In Sec. V we study this transition in detail and we show that it has intriguing universal properties that do not depend essentially neither on the number of particles in the system nor the internal interactions in the mixture. Finally, we conclude in Sec. VI.

II. THE SYSTEM

In our work, we focus on the simplest possible extension of the two-component mixture of fermions to scenarios where interactions with additional third-component particle (impurity) are present. We assume that all the particles have the same mass m , they are confined in the same one-dimensional parabolic trap of frequency Ω , and they mutually interact via zero-range contact interactions in s -wave channel. This implies of course that, due to the Pauli exclusion principle, only interactions between particles from different components do not vanish. Since in our considerations the third component is essentially distinguished, we write the Hamiltonian of the system conveniently as

$$\hat{\mathcal{H}} = \hat{\mathcal{H}}_{AB} + \hat{\mathcal{H}}_C + \hat{\mathcal{H}}_I. \quad (1)$$

In this sum the Hamiltonian $\hat{\mathcal{H}}_{AB}$ describes the two-component mixture of fermions and in the second quantization reads

$$\begin{aligned} \hat{\mathcal{H}}_{AB} = & \int dx \sum_{\sigma} \hat{\Psi}_{\sigma}^{\dagger}(x) \left[-\frac{\hbar^2}{2m} \frac{d^2}{dx^2} + \frac{m\Omega^2}{2} x^2 \right] \hat{\Psi}_{\sigma}(x) \\ & + g_0 \sqrt{\frac{\hbar^3 \Omega}{m}} \int dx \hat{\Psi}_B^{\dagger}(x) \hat{\Psi}_A^{\dagger}(x) \hat{\Psi}_A(x) \hat{\Psi}_B(x). \end{aligned} \quad (2a)$$

Here $\sigma \in \{A, B\}$ enumerates mixture's components while $\hat{\Psi}_{\sigma}(x)$ is a field operator annihilating σ -component particle at position x . These operators obey fermionic anti-commutation relations $\{\hat{\Psi}_{\sigma}(x), \hat{\Psi}_{\sigma'}^{\dagger}(x')\} = \delta_{\sigma\sigma'} \delta(x - x')$ and $\{\hat{\Psi}_{\sigma}(x), \hat{\Psi}_{\sigma'}(x')\} = 0$. Dimensionless parameter g_0 quantifies an effective interaction strength between components.

Contrary, the Hamiltonian $\hat{\mathcal{H}}_C$ describes a third-component particle confined in the same trap. In the first quantization, it is represented by the differential operator of the form

$$\hat{\mathcal{H}}_C = -\frac{\hbar^2}{2m} \frac{d^2}{dz^2} + \frac{m\Omega^2}{2} z^2, \quad (2b)$$

where z is the position of the particle.

Finally, the Hamiltonian $\hat{\mathcal{H}}_I$ is responsible for interactions between the two-component mixture and the third particle. It can be written as

$$\hat{\mathcal{H}}_I = g \sqrt{\frac{\hbar^3 \Omega}{m}} \int dx \sum_{\sigma} \hat{\Psi}_{\sigma}^{\dagger}(x) \delta(x - z) \hat{\Psi}_{\sigma}(x), \quad (2c)$$

where the dimensionless parameter g is the effective interaction strength. Note that we assumed here that interactions with the third-component particle are the same for both components. Generalization to non-symmetric interactions is straightforward but beyond the scope of this work. We treat both interaction strengths g_0 and g

as independent parameters. It is justified from an experimental point since in principle they depend differently on the external magnetic field [38], the shape of the trapping potential in the transverse direction [39], and the channel of interactions determined by the total spin of colliding particles [40].

Let us also underline that in our approach we intentionally use different formalisms for different components, *i.e.*, the two-component mixture is described in the second quantization which automatically takes into account the fermionic statistics, while the third-component particle is described within the first quantization emphasizing that there is only one particle there. In this notation, the total Hamiltonian $\hat{\mathcal{H}}$ acts in the Hilbert space being a tensor product of a single-particle Hilbert space of the third particle and a Fock space in the occupation number representation of the two-component mixture. This formalism has previously been used successfully to describe spinless fermions interacting with single impurity [37].

In the Hamiltonian (1) we already assumed many limiting simplifications: one-dimensionality, an equal mass of all particles, the same parabolic trap, zero-range s -wave interactions, or symmetric interaction with the third component. Still, however, there is a huge flexibility related to the number of particles in components A and B . Fortunately, the Hamiltonian (1) commutes independently with operators of the total number of particles $\hat{N}_{\sigma} = \int dx \hat{\Psi}_{\sigma}^{\dagger}(x) \hat{\Psi}_{\sigma}(x)$. It means that its properties can be studied independently in the subspaces of a well-defined number of particles. It is known that in the case of two-component mixtures (in our case equivalent to setting $g = 0$) measurable properties of the system strongly depend on the particle-number imbalance. This is related to a specific competition between the external potential constantly compressing the cloud of all particles, the quantum statistics acting inside fermionic components acting as quantum repelling pressure, and the inter-component interactions tending to spatially separate different components. To make our analysis as clear as possible, in this work, we focus only on symmetric mixtures having the same number of particles in both components, $N = N_A = N_B$. This assumption, together with the assumption of symmetric interactions with the third-component particle, leads directly to a full symmetry in the mixture sector. This symmetry is manifested formally by the fact that any eigenstate of the many-body Hamiltonian (1) is invariant under the interchange of A and B components.

III. THE METHOD

To find the many-body ground state of the Hamiltonian (1) we adopt the numerically exact diagonalization technique. To make it feasible and accurate we need to

build an appropriately tuned many-body basis in which the Hamiltonian is represented and diagonalized. Since all particles are confined in the same external parabolic potential, it is convenient to choose the eigenstates of the harmonic oscillator as a single-particle basis for all components. They have a known textbook form

$$\varphi_n(z) = (2^n n! \sqrt{\pi a_0})^{-1/2} \mathbf{H}_n\left(\frac{z}{a_0}\right) \exp\left(-\frac{z^2}{2a_0^2}\right), \quad (3)$$

where $\mathbf{H}_n(\cdot)$ is n -th Hermite polynomial and $a_0 = \sqrt{\hbar/m\Omega}$ is a natural unit of length in the problem. These functions are eigenfunctions of the operator (2b) with eigenvalue $E_n = (n + 1/2)\hbar\Omega$. In this way one can decompose field operators and introduce corresponding annihilation operators as

$$\hat{\Psi}_A(x) = \sum_i \hat{a}_i \varphi_i(x), \quad \hat{\Psi}_B(x) = \sum_i \hat{b}_i \varphi_i(x). \quad (4)$$

Of course, they fulfill natural anticommutation fermionic relations. This gives us a natural path to introduce basis in the many-body Hilbert space. As mentioned already, in our notation, the basis vectors have a form of tensor product

$$|\vec{\alpha}, \vec{\beta}, n\rangle = |\phi_n\rangle \otimes \left(a_{\alpha_1}^\dagger \cdots a_{\alpha_N}^\dagger b_{\beta_1}^\dagger \cdots b_{\beta_N}^\dagger |\text{vac}\rangle\right), \quad (5)$$

where $|\phi_n\rangle$ is a state of the third-component particle occupying n -th single-particle orbital, while two integer vectors $\vec{\alpha} = (\alpha_1, \dots, \alpha_N)$ and $\vec{\beta} = (\beta_1, \dots, \beta_N)$ encode single-particle orbitals occupied by individual fermions from components A and B , respectively. Indistinguishability and fermionic nature of particles is guaranteed by imposing additional constraints of the form $\alpha_1 > \alpha_2 > \dots > \alpha_N$ and $\beta_1 > \beta_2 > \dots > \beta_N$. States (5) are obviously eigenstates of the non-interacting Hamiltonian ($g_0 = g = 0$) and have energies $E_{\vec{\alpha}, \vec{\beta}, n} = \hbar\Omega [(2N + 1)/2 + n + \sum_i (\alpha_i + \beta_i)]$. Non-interacting ground state has energy $E_0 = N^2 + 1/2$.

To diagonalize numerically the Hamiltonian one needs to cut the basis. In our approach, we do not perform simple cuts on single-particle excitations but rather we limit the many-body basis to states having total (non-interacting) energy $E_{\vec{\alpha}, \vec{\beta}, n}$ not larger than some fixed energy limit E_C . In this way, we do not exclude from the description low-energy states having only a few particles highly excited, while we neglect high-energy states with many low-excited particles. It was shown in previous studies that such a method gives a much better approximation of interacting many-body states with the same usage of numerical resources [41–44]. Following this procedure, for a given number of particles N and interaction strengths g_0 and g , we represent the Hamiltonian (1) in the truncated many-body basis and diagonalize with the implicitly-restarted Arnoldi-Lanchos algorithm [45]. As

a result we obtain the lowest eigenstates and their energies. Particularly, the many-body ground state $|\mathbf{G}\rangle$ having energy $\mathcal{E}_\mathbf{G}$ is represented as a superposition of basis states

$$|\mathbf{G}\rangle = \sum_{\vec{\alpha}, \vec{\beta}, n} G_{\vec{\alpha}, \vec{\beta}, n} |\vec{\alpha}, \vec{\beta}, n\rangle. \quad (6)$$

Let us mention here that in the case of harmonic confinement further optimization techniques of the many-body basis are possible [46–49]. They are vital when large interaction strengths are considered. In the cases of relatively weak interactions studied in our work, this kind of optimization has limited importance. Therefore, we do not introduce them to our scheme.

IV. IMPACT OF THE IMPURITY

In principle, the impact of interactions with an additional impurity on the system can be analyzed from two complementary perspectives, depending if one is interested in the external or internal behavior of the mixture. First, let us discuss the external features when interactions with the impurity are present. The simplest quantities that feel an influence of additional interaction are single-particle density distributions $n_\sigma(x)$ of mixture components and $m(x)$ of the impurity. They are straightforwardly defined as

$$n_\sigma(x) = \langle \mathbf{G} | \mathbb{1} \otimes \hat{\Psi}_\sigma^\dagger(x) \hat{\Psi}_\sigma(x) | \mathbf{G} \rangle, \quad (7a)$$

$$m(x) = \langle \mathbf{G} | \hat{\mathbb{P}}_x \otimes \mathbb{1} | \mathbf{G} \rangle, \quad (7b)$$

where $\hat{\mathbb{P}}_x = |x\rangle\langle x|$ projects to an eigenstate $|x\rangle$ of position operator. Of course, due to the exchange symmetry $A \leftrightarrow B$ explained before, both density distributions $n_A(x)$ and $n_B(x)$ are exactly the same. In Fig. 1(a), we present these distributions (thick blue and thin red lines) for the system of five particles ($N = 2$) for different interaction strengths g , keeping fixed internal interaction $g_0 = 1$. For better comparison, we additionally display with the shadowed area the non-interacting ($g_0 = g = 0$) distribution $n_\sigma(x)$. It is clear that along with increasing g , the distribution of the impurity $m(x)$ significantly changes its character and for sufficiently large repulsions it is split and pushed out from the center where the mixture is concentrated. In contrast, distributions of mixture components $n_\sigma(x)$ are only slightly affected. This behavior of density distributions can be investigated further by considering the two-particle density distribution

$$\mu_\sigma(x, z) = \langle \mathbf{G} | \hat{\mathbb{P}}_z \otimes \hat{\Psi}_\sigma^\dagger(x) \hat{\Psi}_\sigma(x) | \mathbf{G} \rangle \quad (8)$$

which encodes the joint probability of finding the impurity at position z and one of the particles from the component σ at position x . The distribution for the same parameters of the system is shown in Fig. 1(b). In addition

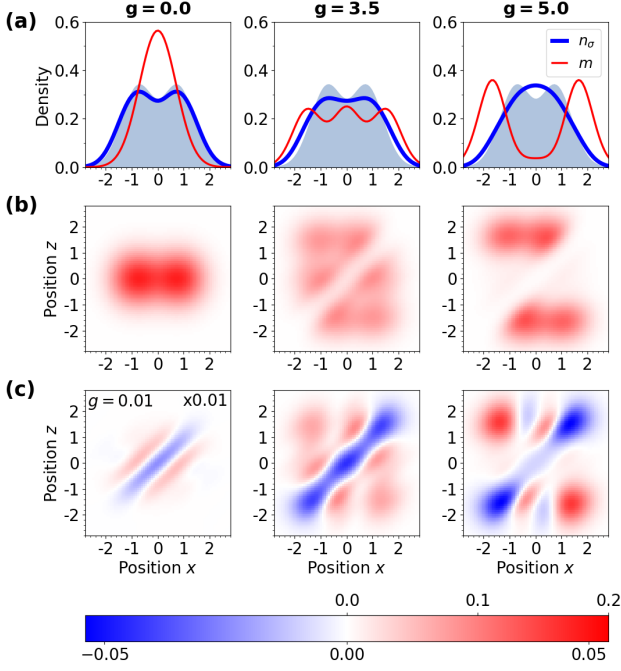


FIG. 1. Impact of interactions with the third-component particle on the two-component mixture containing four particles ($N = 2$). Different columns correspond to different values of interaction strength with the impurity g . In all plots, inter-component interaction strength is fixed, $g_0 = 1$. (a) Single-particle density profiles of the mixture's components $n_\sigma(x)$ (thick blue) and the third-component particle $m(x)$ (thin red). For a better comparison, the non-interacting distribution of the mixture's components is additionally displayed with a light blue shadow. (b) Two-particle density profile $\mu_\sigma(x, z)$. (c) Distribution of correlations $\mathcal{G}_\sigma(x, z)$ between impurity and particle from the component σ . Note, that in the left plot, we consider the interaction strength g slightly positive ($g = 0.01$) since for vanishing interactions the distribution vanishes. In this case, the distribution intensity is also scaled by a factor 10^2 to make it visible. In all plots, positions are expressed in units of a_0 . The upper and lower values on the color bar refer to plots (b) and (c), respectively.

to the spatial separation already deduced from single-particle distributions, the two-particle density clearly indicates that some correlations between mixture and impurity are developed. Most significantly they are visible along the diagonal direction $z = x$, *i.e.*, the probability of finding both particles at the same position quickly vanishes with increasing interaction g . Of course, this effect cannot be captured by single-particle distributions and is not present in the direct product $n_A(x)m(z)$. To make it evident we additionally display in Fig. 1(c) the distribution of correlations defined as

$$\mathcal{G}_\sigma(x, z) = \mu_\sigma(x, z) - n_\sigma(x)m(z). \quad (9)$$

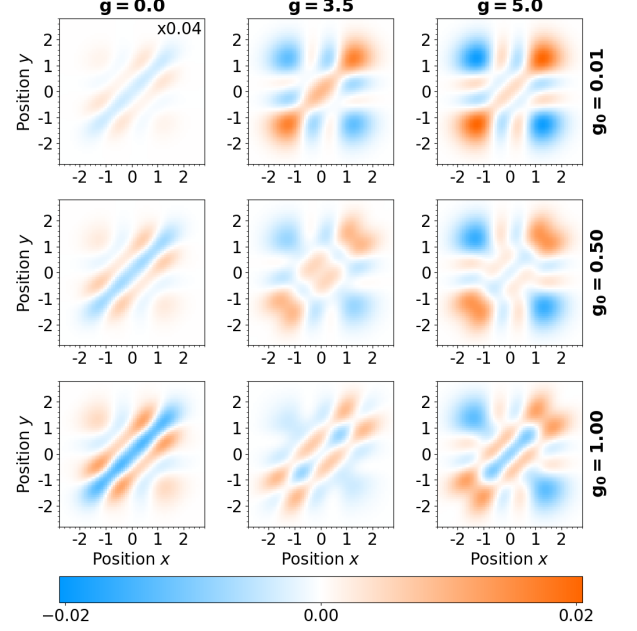


FIG. 2. Distribution of internal two-particle correlations $\mathcal{K}(x, y)$ for the system of five particles ($N = 2$) for different internal interaction strengths g_0 and interactions with the impurity g . For any fixed interaction g_0 , along with increasing repulsion g , the transition between two different regimes is visible. In all plots, positions are expressed in units of a_0 .

Its negative (positive) value indicates that the actual probability is smaller (higher) than the probability that would result from the assumption of complete independence of the components.

From the perspective of the internal properties of the mixture, the description is slightly simpler. As noticed already, interactions with the impurity do not influence significantly the single-particle distribution of the mixture. It turns out that this is also the case when one considers the inter-component two-particle distribution

$$\nu(x, y) = \langle \mathbf{G} | \hat{\mathbf{1}} \otimes \hat{\Psi}_A^\dagger(x) \hat{\Psi}_A(x) \hat{\Psi}_B^\dagger(y) \hat{\Psi}_B(y) | \mathbf{G} \rangle. \quad (10)$$

The impact of the impurity is however noticeable when the distribution of two-particle correlations is analyzed. It is defined analogously to correlations (9) as

$$\mathcal{K}(x, y) = \nu(x, y) - n_A(x)n_B(y). \quad (11)$$

In Fig. 2 we show this distribution for different values of interactions g_0 and g for the same system of five particles ($N = 2$). The magnitude of correlations is very small when compared to the magnitude of correlations in $\mathcal{G}_\sigma(x, z)$. However, in the region of parameters where the impurity starts to leak outside the mixture, its structural transition is clearly visible.

Up to now, we presented illustrative results for a system containing five particles (two particles in each mixture's component and the impurity). For completeness,

we performed analogous calculations for systems with a larger number of particles in the mixture (up to $N = 5$). They are exposed in the Supplemental Material [50]. On a quantitative level, the results obtained are very similar in the sense that the observed structural change in the many-body ground state is universal. Namely, for a given number of particles and fixed internal interaction g_0 , one finds such interaction strength g at which distributions change rapidly. Particularly, the single-particle density $m(x)$ is split and pushed to the edges while the distribution of internal correlations $\mathcal{K}(x, y)$ changes its nature.

From phenomenological argumentation, some kind of separation of the components is suspected. When interactions are strong enough the single-particle excitations become energetically favourable over interaction energy cost. Then, to reduce the overlap of the densities the system excites particles. It should be noted, however, that the separation observed here is substantially different from separations observed in systems of single-component fermions interacting with the impurity [51]. It was shown that in those systems, the impurity remains in the middle of the trap while the fermionic component is (only slightly) split and pushed out from the center. In our case, although repulsive interactions in the fermionic mixture are present, the distribution of the impurity is split and driven to the edges. As noted in the literature, in the case of the single-component Fermi sea, the existence of this kind of separation requires a noticeable mass difference between impurity and other particles [37, 52].

V. THE STRUCTURAL TRANSITION

As explained already, the system studied experiences some substantial transition in its many-body ground state, and a precise quantitative study of its nature is needed. To get a better understanding of this transition we utilize additional quantitative tools. Since the method of exact diagonalization gives direct access to the structure of the many-body ground state one can calculate the fidelity between ground states obtained for different interaction strengths. When internal interaction g_0 is fixed, the fidelity is defined as

$$\mathcal{F}(g_0; g_1, g_2) = |\langle \mathbf{G}(g_0, g_1) | \mathbf{G}(g_0, g_2) \rangle|^2, \quad (12)$$

where we explicitly mark that the many-body ground state $|\mathbf{G}(g_0, g)\rangle$ is calculated for interactions g_0 and g , respectively. Since for $g_1 = g_2$ the fidelity is extreme and equal to 1, one expands it naturally into the series

$$\mathcal{F}_{g_0}(g_1, g_2) = 1 - \chi(g_0; g_1)(g_2 - g_1)^2 + \dots \quad (13)$$

In this expansion $\chi(g_0; g) = \partial_{g'}^2 \mathcal{F}(g_0; g, g')|_{g'=g}$ is the fidelity susceptibility which quantifies resistivity of the ground state on infinitesimal change of interaction

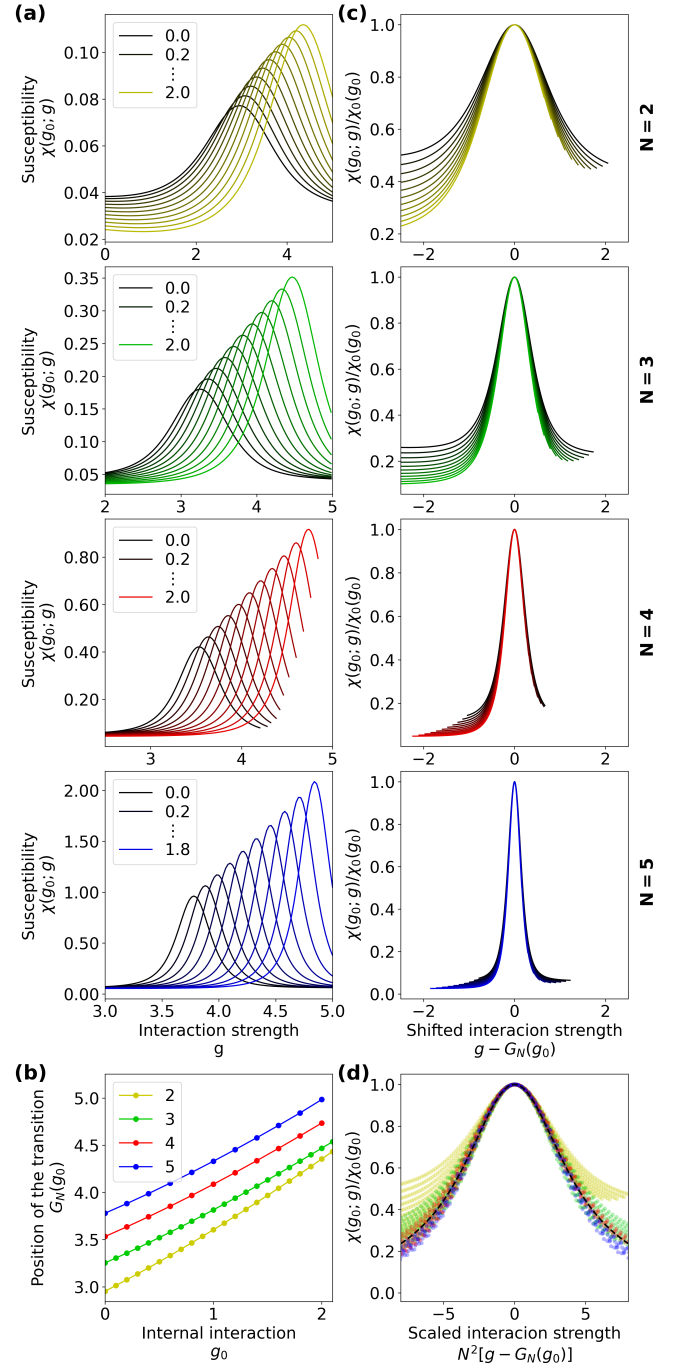


FIG. 3. Properties of the fidelity susceptibility for different numbers of particles in the system. **(a)** The fidelity susceptibility $\chi(g_0; g)$ as a function of interaction g for different internal interactions g_0 . **(b)** Position of the transition $G_N(g_0)$ as a function of internal interaction g_0 . **(c)** Susceptibilities from the left plot after rescaling in magnitude by $\chi_0(g_0)$ and centering around the transition interaction $G_N(g_0)$. All plots collapse to the same universal curve signaling the specific universality of the transition. **(d)** Numerical collapse to the universal curve Φ (dashed black) of all the fidelity susceptibility curves (different points and colors) after applying appropriate scaling (15). Note that deviations from the universality are diminished when the number of particles in the mixture increases.

strength [53, 54]. Its large amplitude for a given value of g signals that at this point the ground state of the system rapidly changes with g , *i.e.*, the state of the system quickly moves toward different regions of the Hilbert space.

In Fig. 3(a) we present the susceptibility $\chi(g_0; g)$ as a function of interaction with the impurity g for different internal interactions g_0 . Successive rows correspond to varying numbers of particles in the mixture N . It is clear that the position of the transition $G_N(g_0)$, *i.e.*, interaction strength g for which the susceptibility is maximal (Fig. 3(b)), depends monotonically on the internal interaction in the mixture g_0 . The intensity of the transition (magnitude of the susceptibility) is evidently higher for systems with a larger number of particles. Contrary, the shape of the function $G_N(g)$ is not strongly affected by the number of particles.

One of the most interesting properties of the observed transition is its remarkable universality. It is easily recognized with an appropriate rescaling of the susceptibility function. To make it evident, in Fig. 3(c), we plot susceptibilities as a function of distance from the transition point $\tau = g - G_N(g_0)$ and normalized to its maximal value $\chi_0(g_0) = \chi(g_0; G_N(g_0))$. We find then that, in the vicinity of the transition, all the susceptibility curves obtained for a given number of particles N follow a single universal distribution $\phi_N(\xi)$. Of course, with increasing distance from the transition point, the curves determined for different g_0 become increasingly different from the universal shape. Note, however, that these deviations are diminished when the number of particles in the mixture is increased. This observation suggests that for any internal interaction strength g_0 the susceptibility can be written as

$$\chi(g_0; g) = \chi_0(g_0) \cdot \phi_N(g - G_N(g_0)). \quad (14)$$

In principle, the N -dependent universal curve $\phi_N(\xi)$ is different for different numbers of particles in the mixture. For example, it is visible that for a larger number of particles, it becomes significantly narrower, indicating that the transition is more rapid. We found, however additional simple scaling between systems of different numbers of particles which makes all the curves reasonably overlapping. Namely, all N -dependent functions $\phi_N(\xi)$ can be fused to a single universal curve $\Phi(\xi)$ by applying the scaling $\phi_N(\xi) = \Phi(N^2\xi)$. In Fig. 3(d), we display all the fidelity susceptibilities from panel (a) after the aforementioned scaling and shifting. We see that all the transition plots follow almost the same curve, and the agreement is better for a larger number of particles. Consequently, we argue that any fidelity susceptibility curve can be derived straightforwardly from the universal function $\Phi(\xi)$ via the relation

$$\chi(g_0; g) = \chi_0(g_0) \cdot \Phi(N^2(g - G_N(g_0))). \quad (15)$$

The observed scaling with the number of particles in the mixture is of course a direct consequence of the scaling of the interaction energy (the impurity interacts mutually with N^2 particles in the mixture). From this perspective, all susceptibility curves are identical. This also indirectly explains why the scaling found becomes better with an increase in the number of particles.

Let us underline here that the shape of the universal curve $\Phi(\xi)$ is not known and probably cannot be deduced with any simple heuristic arguments. However, it turns out that it can be well approximated by a simple one-parameter Lorentzian shape of the form

$$\Phi(\xi) = \frac{\Gamma_0^2}{\xi^2 + \Gamma_0^2}. \quad (16)$$

The numerical fit to all the data (for $N > 2$) gives $\Gamma_0 \approx 4.34$ and the resulting shape is presented in Fig. 3(d) with a dashed black line. The observed universality of the structural transition, and its simple scaling with particle number, suggests that the transition is driven rather by a collective mechanism that is only weakly influenced by the microscopic properties of individual particles.

Lastly, it should be emphasized that the universality just described is a feature for systems where the number of particles in the mixture is large. Indeed, as already mentioned, for small N deviations from the universal curve are evident. Moreover, we checked that for a system of three particles, *i.e.*, a single particle in each component ($N = 1$), discrepancies are huge and claiming any universality is not justified.

VI. CONCLUSIONS

In our work, we extensively investigated the ground-state properties of the simplest three-component fermionic mixtures, *i.e.*, a balanced two-component mixture interacting additionally with a single impurity from the third flavor. By applying the method of exact diagonalization, we access not only the ground-state energy and density profiles of particular components but also the mutual correlations existing in the system. We observed that with increasing interaction with the impurity, a specific ground-state transformation occurs in the system, during which the third component (the impurity) is split and pushed to the edges of the system. Although the interaction strength at which the transition occurs depends on the number of particles and internal interactions in the mixture, it has many universal features. In particular, the shape of the susceptibility curve does not depend (after taking into account the scaling of interactions) on the internal parameters of the mixture.

Our work is the next step towards a better understanding of the properties of imbalanced multi-component mixtures of several strongly correlated ultracold fermions.

The observed transition and its universality show that a detailed analysis of such systems can expose many of their interesting properties that have no counterparts in systems with fewer components. There are two natural directions for extending our work. One is to consider interactions of the impurity with balanced mixtures of more than two components. The other is to consider interactions with more than one impurity with a multi-component mixture and explore substantial differences with earlier results for a spinless Fermi sea [55].

DATA AVAILABILITY STATEMENT

All numerical data presented in this paper and additional figures for different numbers of particles in the mix-

ture are available online [50].

ACKNOWLEDGMENTS

This research was supported by the National Science Centre (NCN, Poland) within the OPUS project No. 2023/49/B/ST2/03744. For the purpose of Open Access, the authors have applied a CC-BY public copyright licence to any Author Accepted Manuscript version arising from this submission.

-
- [1] P. Kapitza, *Nature* **141**, 74 (1938).
 - [2] J. F. Allen and A. D. Misener, *Nature* **142**, 643 (1938).
 - [3] H. K. Onnes, *Commun. Phys. Lab. Univ. Leiden* **12**, 120 (1911).
 - [4] J. Bardeen, L. N. Cooper, and J. R. Schrieffer, *Phys. Rev.* **108**, 1175 (1957).
 - [5] H. L. Stormer, D. C. Tsui, and A. C. Gossard, *Rev. Mod. Phys.* **71**, S298 (1999).
 - [6] M. N. Baibich, J. M. Broto, A. Fert, F. N. Van Dau, F. Petroff, P. Etienne, G. Creuzet, A. Friederich, and J. Chazelas, *Phys. Rev. Lett.* **61**, 2472 (1988).
 - [7] G. Binasch, P. Grünberg, F. Saurenbach, and W. Zinn, *Phys. Rev. B* **39**, 4828 (1989).
 - [8] A. Georges, G. Kotliar, W. Krauth, and M. J. Rozenberg, *Rev. Mod. Phys.* **68**, 13 (1996).
 - [9] F. Dalfovo, S. Giorgini, L. P. Pitaevskii, and S. Stringari, *Rev. Mod. Phys.* **71**, 463 (1999).
 - [10] M. Bender, P.-H. Heenen, and P.-G. Reinhard, *Rev. Mod. Phys.* **75**, 121 (2003).
 - [11] R. O. Jones, *Rev. Mod. Phys.* **87**, 897 (2015).
 - [12] M. E. Fisher, *Rev. Mod. Phys.* **70**, 653 (1998).
 - [13] Y. Murayama, *Mesoscopic Systems: Fundamentals and Applications* (Wiley-VCH, Weinheim, 2001).
 - [14] P. Cheinet, S. Trotzky, M. Feld, U. Schnorrberger, M. Moreno-Cardoner, S. Fölling, and I. Bloch, *Phys. Rev. Lett.* **101**, 090404 (2008).
 - [15] F. Serwane, G. Zürn, T. Lompe, T. B. Ottenstein, A. N. Wenz, and S. Jochim, *Science* **332**, 336 (2011).
 - [16] A. N. Wenz, G. Zürn, S. Murmann, I. Brouzos, T. Lompe, and S. Jochim, *Science* **342**, 457 (2013).
 - [17] D. Blume, *Reports on Progress in Physics* **75**, 046401 (2012).
 - [18] Zinner, Nikolaj Thomas, *EPJ Web of Conferences* **113**, 01002 (2016).
 - [19] T. Sowiński and M. Ángel García-March, *Reports on Progress in Physics* **82**, 104401 (2019).
 - [20] M. Holten, L. Bayha, K. Subramanian, S. Brandstetter, C. Heintze, P. Lunt, P. M. Preiss, and S. Jochim, *Nature* **606**, 287 (2022).
 - [21] E. K. Laird, B. C. Mulkerin, J. Wang, and M. J. Davis, *SciPost Phys.* **17**, 163 (2024).
 - [22] M. Gajda, J. Mostowski, T. Sowiński, and M. Załuska-Kotur, *Europhysics Letters* **115**, 20012 (2016).
 - [23] M. Holten, L. Bayha, K. Subramanian, C. Heintze, P. M. Preiss, and S. Jochim, *Phys. Rev. Lett.* **126**, 020401 (2021).
 - [24] M. A. Cazalilla and A. M. Rey, *Reports on Progress in Physics* **77**, 124401 (2014).
 - [25] G. Pagano, M. Mancini, G. Cappellini, P. Lombardi, F. Schäfer, H. Hu, X.-J. Liu, J. Catani, C. Sias, M. Inguscio, and L. Fallani, *Nature Physics* **10**, 198 EP (2014).
 - [26] L. Sonderhouse, C. Sanner, R. B. Hutson, A. Goban, T. Bilitewski, L. Yan, W. R. Milner, A. M. Rey, and J. Ye, *Nature Physics* **16**, 1216 (2020).
 - [27] X.-J. Liu, H. Hu, and P. D. Drummond, *Phys. Rev. A* **77**, 013622 (2008).
 - [28] Y. Jiang, J. Cao, and Y. Wang, *Europhysics Letters* **87**, 10006 (2009).
 - [29] X. W. Guan, J.-Y. Lee, M. T. Batchelor, X.-G. Yin, and S. Chen, *Phys. Rev. A* **82**, 021606 (2010).
 - [30] J. Y. Lee, X. W. Guan, and M. T. Batchelor, *Journal of Physics A: Mathematical and Theoretical* **44**, 165002 (2011).
 - [31] C. C. N. Kuhn and A. Foerster, *New Journal of Physics* **14**, 013008 (2012).
 - [32] X.-W. Guan, Z.-Q. Ma, and B. Wilson, *Phys. Rev. A* **85**, 033633 (2012).
 - [33] Y. Jiang, P. He, and X.-W. Guan, *Journal of Physics A: Mathematical and Theoretical* **49**, 174005 (2016).
 - [34] E. K. Laird, Z.-Y. Shi, M. M. Parish, and J. Levinsen, *Phys. Rev. A* **96**, 032701 (2017).
 - [35] J. Dobrzyniecki and T. Sowiński, *Advanced Quantum Technologies* **3**, 2000010 (2020).
 - [36] J. Silva-Valencia and J. J. Mendoza-Arenas, *Phys. Rev. A* **111**, 053316 (2025).
 - [37] D. Włodzyński, *Phys. Rev. A* **106**, 033306 (2022).
 - [38] C. Chin, R. Grimm, P. Julienne, and E. Tiesinga, *Rev. Mod. Phys.* **82**, 1225 (2010).

- [39] M. Olshanii, *Phys. Rev. Lett.* **81**, 938 (1998).
- [40] J. Xu, T. Feng, and Q. Gu, *Annals of Physics* **379**, 175 (2017).
- [41] T. Haugset and H. Haugerud, *Phys. Rev. A* **57**, 3809 (1998).
- [42] M. Płodzień, D. Wiater, A. Chrostowski, and T. Sowiński, (2018), [arXiv:1803.08387](https://arxiv.org/abs/1803.08387) [cond-mat.quant-gas].
- [43] A. Chrostowski and T. Sowiński, *Acta Physica Polonica A* **136**, 566–570 (2019).
- [44] A. Rojo-Francàs, F. Isaule, and B. Juliá-Díaz, *Phys. Rev. A* **105**, 063326 (2022).
- [45] R. B. Lehoucq, D. C. Sorensen, and C. Yang, *ARPACK Users' Guide* (Society for Industrial and Applied Mathematics, 1998).
- [46] Volosniev, A.G., Fedorov, D.V., Jensen, A.S., and Zinner, N.T., *Eur. Phys. J. Special Topics* **224**, 585 (2015).
- [47] Bellotti, Filipe F., Dehkharghani, Amin S., and Zinner, Nikolaj T., *Eur. Phys. J. D* **71**, 37 (2017).
- [48] P. Kościk, *Physics Letters A* **382**, 2561 (2018).
- [49] P. Kościk, *Few-Body Systems* **61**, 13 (2020).
- [50] M. Teske and T. Sowiński, "Supplemental Material for "Impurity immersed in two-component few-fermion mixture in one-dimensional harmonic trap"," Zenodo (2025).
- [51] E. J. Lindgren, J. Rotureau, C. Forssén, A. G. Volosniev, and N. T. Zinner, *New Journal of Physics* **16**, 063003 (2014).
- [52] D. Pęczak, M. Gajda, and T. Sowiński, *New Journal of Physics* **18**, 013030 (2016).
- [53] W.-L. You, Y.-W. Li, and S.-J. Gu, *Phys. Rev. E* **76**, 022101 (2007).
- [54] L. Wang, Y.-H. Liu, J. Imriška, P. N. Ma, and M. Troyer, *Phys. Rev. X* **5**, 031007 (2015).
- [55] S. I. Mistakidis, G. C. Katsimiga, G. M. Koutentakis, and P. Schmelcher, *New Journal of Physics* **21**, 043032 (2019).